Eur Radiol (2013) 23:1059–1066
DOI 10.1007/s00330-012-2666-0

MAGNETIC RESONANCE

First-pass contrast-enhanced renal MRA at 7 Tesla: initial results

L. Umutlu · S. Maderwald · S. Kinner · O. Kraff · A. K. Bitz · S. Orzada · S. Johst · K. Wrede · M. Forsting · M. E. Ladd · T. C. Lauenstein · H. H. Quick

Received: 3 July 2012 / Revised: 28 August 2012 / Accepted: 8 September 2012 / Published online: 14 October 2012

Abstract
Objective The aim of this study was to assess the feasibility of first-pass contrast-enhanced renal MR angiography (MRA) at 7 T.
Methods In vivo first-pass contrast-enhanced high-field examinations were obtained in eight healthy subjects on a 7-T whole-body MRI. A custom-built body transmit/receive radiofrequency (RF) coil and RF system suitable for RF shimming were used for image acquisition. For dynamic imaging, gadobutrol was injected intravenously and coronal unenhanced, arterial and venous data sets using a T1-weighted spoiled gradient-echo sequence were obtained. Qualitative image analysis and assessment of artefact impairment were performed by two senior radiologists using a five-point scale (5 = excellent, 1 = non-diagnostic). SNR and CNR of the perirenal abdominal aorta and both main renal arteries were assessed.
Results Qualitative image evaluation revealed overall high-quality delineation of all assessed segments of the unenhanced arterial vasculature ($mean_{unenhanced}$ 4.13). Nevertheless, the application of contrast agent revealed an improvement in vessel delineation of all the vessel segments assessed, confirmed by qualitative ($mean_{unenhanced}$ 4.13 to $mean_{contrast\text{-}enhanced}$ 4.85) and quantitative analysis (SNR $mean_{unenhanced}$ 64.3 to $mean_{contrast\text{-}enhanced}$ 98.4).
Conclusion This study demonstrates the feasibility and current constraints of ultra-high-field contrast-enhanced renal MRA relative to unenhanced MRA.
Key Points
- *First-pass contrast-enhanced renal MRA at 7 T is technically feasible.*
- *Unenhanced renal MRA offers inherent hyperintense delineation of renal arterial vasculature.*
- *Contrast media application improves vessel assessment of renal arteries at 7 T.*

Keywords MR angiography · Renal MRA · Ultra-high-field MRA · 7 T MR imaging · First-pass contrast-enhanced MRA

L. Umutlu · S. Maderwald · S. Kinner · O. Kraff · A. K. Bitz · S. Orzada · S. Johst · K. Wrede · M. Forsting · M. E. Ladd · T. C. Lauenstein · H. H. Quick
Erwin L. Hahn Institute for Magnetic Resonance Imaging, University Duisburg-Essen, Arendahls Wiese 199, 45141 Essen, Germany

L. Umutlu (✉) · S. Maderwald · S. Kinner · O. Kraff · A. K. Bitz · S. Orzada · S. Johst · M. Forsting · M. E. Ladd · T. C. Lauenstein · H. H. Quick
Department of Diagnostic and Interventional Radiology and Neuroradiology, University Hospital Essen, Hufelandstr. 55, 45122 Essen, Germany
e-mail: Lale.Umutlu@uk-essen.de

K. Wrede
Department of Neurosurgery, University Hospital Essen, Hufelandstr. 55, 45122 Essen, Germany

H. H. Quick
Institute of Medical Physics, Friedrich-Alexander-University Erlangen-Nuernberg, Henkestr. 91, 91502 Erlangen, Germany

Introduction

Contrast-enhanced (CE) magnetic resonance angiography (MRA) has emerged to become an excellent non-invasive diagnostic alternative for the assessment of renal arterial lesions [1]. Multiple trials have proven the superior diagnostic accuracy of CE-MRA in comparison to ultrasound [2] and unenhanced

MR angiography [3] techniques as well as its diagnostic equivalence to computed tomography angiography (CTA) [4] and digital subtraction angiography (DSA) [1].

The increase in the magnetic field strength from 1.5 T (T) to 3 T has been demonstrated to be beneficial for abdominal MRA, mostly because of the increased signal-to-noise ratio (SNR) as well as the higher sensitivity to T1-shortening contrast agents [5]. However, a further increase in the field strength beyond 3 T is likely to yield potential disadvantages for abdominal imaging including angiographic applications. Initial studies with renal and liver MRI at 7 T [6–8] have demonstrated potential benefits but also challenges in imaging abdominal structures at ultra-high magnetic field strength, mostly because of impairments by RF heterogeneities attributable to the shortening of the wavelength. Furthermore, initial approaches in 7-T neuro and abdominal imaging displayed a homogeneous hyperintense signal intensity of unenhanced arterial vasculature in T1-weighted imaging [6, 9]. Starting out as an incidental finding, this observation provoked the idea of unenhanced angiographic high-field applications. Metzger et al. recently revealed preliminary study results demonstrating the feasibility and potential of unenhanced renal MRA at 7 T [10]. However, the feasibility of contrast-enhanced MR angiographic application at 7 T has not yet been investigated.

Hence, the aim of this trial was to assess the feasibility of 7-T contrast-enhanced high-field MRA of the renal vasculature and evaluate the potential benefit of the application of gadolinium-based contrast agents.

Materials and methods

Study population

Eight healthy volunteers (5 female, 3 male; average age 29.5 years, range 21–39 years) were enrolled in this trial. Study procedures were conducted in accordance with all guidelines set forth by the approving institutional review board and informed consent was obtained before each examination.

MRI and coil system

All examinations were performed in the head-first, supine position on a 7-T whole-body MRI (Magnetom 7 T, Siemens Healthcare Sector, Erlangen, Germany) equipped with a high-performance gradient system providing a strength of 38 mT/m and a maximum slew rate of 170 mT/m/ms.

A custom-built transmit/receive RF coil was utilised. To ensure improved intrinsic coil decoupling as well as larger RF penetration depth and the best possible B1 uniformity, the coil was built of eight symmetrically excited meander strip line elements enclosed in special modules. The coil was built of two arrays (with four elements each) placed on the ventral and dorsal upper half of the abdomen (Fig. 1) [11]; the ventral elements were interconnected with a flexible neoprene sheet.

A custom-built, add-on eight-channel RF system was applied for static RF shimming to reduce B_1 field heterogeneities associated with the shortened Larmor wavelength at ultra-high field strength [12]. B_0 shimming was performed in the region of interest (ROI), defined as the perirenal aorta and both renal arteries. Fixed amplitude and phase settings for the custom eight-channel RF coil were applied utilising equal amplitudes and a phase increment of 45° between neighbouring elements (conventional CP^+ mode) to transition the B1 signal voids out of the ROI to the right upper quadrant of the abdomen.

SAR calculations were performed in advance in two human body models from the Virtual Family [13] (Duke, 70 kg, male, 1.74 m; Ella, 58 kg, female, 1.6 m; Hugo, 95 kg male, 1.85 m), yielding maximum permissible input power levels in compliance with the IEC safety guidelines (10 W/kg for 10 g-averaged local SAR) of 65 W for imaging of a male subject with body physique similar to Duke and 58 W for imaging of a female subject similar to Ella, respectively.

Sequence optimisation and imaging

When transitioning from lower magnetic field strengths to ultra-high-field imaging, sequences and examination

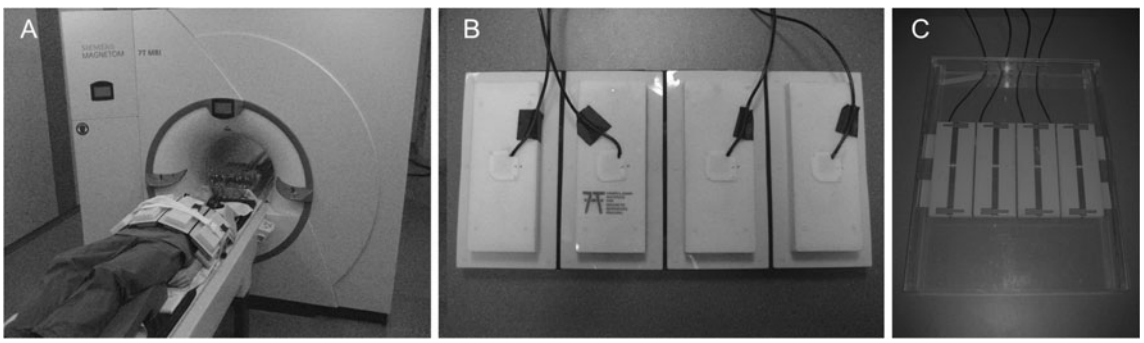

Fig. 1 **a** Seven-Tesla whole-body MRI. **b** Ventral and **c** dorsal components of the eight-channel transmit/receive RF array

protocols need adjustments and modifications with regard to SAR constraints and altered T1 relaxation times to provide the best possible image quality. Hence, imaging parameters (e.g. repetition time [TR], echo time [TE], and flip angle [α]) were adopted with application of the shortest achievable TE and TR and best contrast. Due to the strong flip angle variation in 7-T trunk images, the flip angle was consecutively adapted within the SAR limits for a given TE/TR setting to obtain the best contrast and workflow (no pauses to cool down were included, as may be requested from the SAR supervision). This took place in pilot tests and all eight subjects were imaged with identical parameters. As dynamic imaging demands repeated consecutive measurements, sequence parameters of the coronal T1-weighted spoiled gradient-echo sequence (3D FLASH) were chosen to provide full organ and vessel coverage within a breath hold acquisition time of 20 s. Imaging parameters were as follows: TR 2.98 ms, TE 0.97 ms, field-of-view 400×400 mm^2, bandwidth 450 Hz/pixel, nominal flip angle 25°, and 269×384 matrix interpolated to 538×768, resulting in an uninterpolated in-plane resolution of 1.5×1.0 mm^2 with a slice thickness of 1.0 mm. Parallel imaging was performed with the generalised auto-calibrating, partially parallel acquisition algorithm (GRAPPA) with an acceleration factor of 2 with 24 reference lines.

In four out of the eight subjects, two sinc-shaped 90° RF pulses that are commonly used for saturation of venous signal were placed above and below the imaging slab before the acquisition of the actual dynamic sequence to saturate the hyperintense signal of both the the arterial and venous vasculature and thus to optimise the vessel signal in the subtraction images. To reduce the SAR contribution of the two pulses, the variable-rate selective excitation (VERSE) algorithm was applied [14]. However, diverse approaches remained unsatisfying, as only the signal of the upper and lower portions of the abdomen could be partially saturated, leaving the arterial vessel signal still hyperintense (Fig. 2). Thus, to ensure a clean comparison, non-saturated data sets (non-enhanced and contrast-enhanced) were obtained in all eight subjects and accordingly used for qualitative and quantitative evaluation.

For clean quantitative analysis of a potential signal increase after the application of contrast media, an unenhanced coronal T1-weighted spoiled gradient-echo sequence (3D FLASH) was obtained before the intravenous (i.v.) administration of a 1-ml test bolus for determination of the exact arrival time of the contrast agent. Subsequently, arterial (approximately 20 s post i.v.) and venous (approximately 50 s post i.v.) coronal 3D FLASH data sets were obtained. For contrast-enhanced imaging, 0.1 mmol/kg gadobutrol (Gadovist®, Bayer HealthCare Pharmaceuticals, Berlin, Germany), followed by a saline flush of 20 ml, was injected intravenously at 2 ml/s using an automated injector (EmpowerMR®, ACIST Medical Systems, Eden Prairie, MN, USA). Subtraction images were obtained manually after the examination.

Qualitative and quantitative image analysis

All MR images were assessed on a standard Picture Archiving and Communication System (PACS) workstation (Centricity RIS 4.0i, GE Healthcare, Barrington, NJ, USA).

Qualitative image analysis was evaluated in consensus by two radiologists (6 and 10 years of experience with MRA). The quality of vessel delineation was analysed for the unenhanced and arterially enhanced data sets for a total of five predefined vessel segments: (1) abdominal aorta, (2) proximal right renal artery, (3) distal right renal artery, (4) proximal left renal artery, and (5) distal left renal artery. Image quality was rated on a five-point scale with 5 = excellent, 4 = good, 3 = moderate, 2 = poor, and 1 = non-diagnostic vessel delineation. The presence of artefacts, including (1) chemical shift, (2) B_1 heterogeneity, (3) susceptibility, and (4) motion artefacts as well as the (5) overall image impairment, was rated using a dedicated five-point scale (5 = no artefact present/non-significant, 4 = minor artefacts, 3 = moderate impairment, 2 = strong

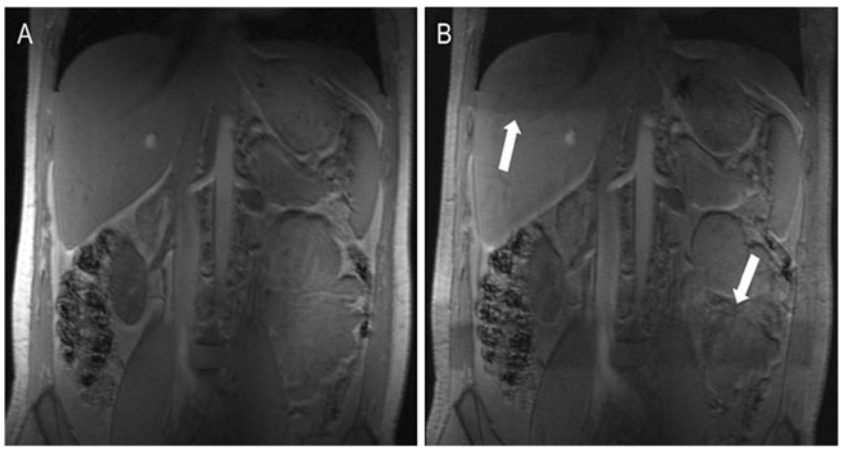

Fig. 2 **a** Hyperintense signal of the arterial vasculature without RF saturation pulses. **b** Slight saturation in the upper portion of the abdomen as well as above the iliac crest (*arrows*). Nevertheless, the hyperintense signal of the arterial vasculature remains equivalent to non-saturated imaging owing to insufficient saturation of inflowing blood

impairment, 1 = non-diagnostic). Score values for image quality and presence of artefacts were compared for each sequence.

For quantitative image analysis, signal-to-noise ratios (SNR_{vessel} = $signal_{vessel}$/noise) and contrast-to-noise ratios [CNR = ($signal_{vessel}$ − $signal_{surrounding\ tissue}$)/noise] of the perirenal abdominal aorta and both main renal arteries in correlation with the adjacent psoas major muscle were measured for all sequences. Noise was defined as the standard deviation of signal in air and was measured extracorporeally. The predefined ROIs were of identical size and placed in identical positions on all images of each volunteer to minimise spatial variation effects.

To assess potential statistically significant changes in qualitative and quantitative analysis, a Wilcoxon rank test was applied, with p-values <0.05 designating statistical significance.

Results

Examinations were successfully performed and well tolerated by all subjects, and no side effects associated with the ultra-high field strength or the application of contrast agent were noted. The average examination time amounted to 28 min (±6 min) including patient positioning, shimming and data acquisition.

Qualitative analysis

Qualitative image evaluation revealed overall high-quality delineation of all assessed segments of the unenhanced arterial vasculature ($mean_{unenhanced}$ 4.13) (Fig. 3A1–A5). Scores ranged from the highest values for the depiction of the abdominal aorta ($mean_{unenhanced}$ 4.59) and proximal left renal artery ($mean_{unenhanced}$ 4.50) to the lowest scores for assessment of the proximal right renal artery ($mean_{unenhanced}$ 3.48).

The application of contrast agent yielded an improvement in the delineation of all the vessel segments assessed, showing an increase in the mean score from unenhanced MRA of 4.13 to 4.79 for contrast-enhanced imaging (Figs. 3, 4). The strongest improvement in vessel delineation with contrast-enhanced imaging was rated for the assessment of the proximal ($mean_{unenhanced}$ 3.48 to $mean_{contrast\text{-}enhanced}$ 4.45) and distal ($mean_{unenhanced}$ 3.79 to $mean_{contrast\text{-}enhanced}$ 4.80) right renal artery (Fig. 5). As the delineation of the unenhanced abdominal aorta and the proximal left renal artery received excellent scores in unenhanced imaging (4.59 and 4.50), the application of contrast agent led to only a mild increase in vessel delineation (4.89 and 4.93, respectively).

Despite the improved assessment of vessel delineation after the application of a contrast agent, no statistically significant changes could be detected in any assessed vessel segment.

Quantitative analysis

In correspondence with the qualitative analysis scores, SNR measurement revealed a fairly high hyperintense signal intensity of the unenhanced arterial vasculature, nevertheless showing a strong yet non-significant increase after the application of contrast agent with an average increase of 34.9 % for all the vessel segments assessed. The strongest increase was detected for the distal segments of the left renal artery ($mean_{unenhanced}$ 59.3 to $mean_{contrast\text{-}enhanced}$ 105.8) (Fig. 6). An equal increase in SNR was detected for the proximal segments of the left renal artery (mean increase

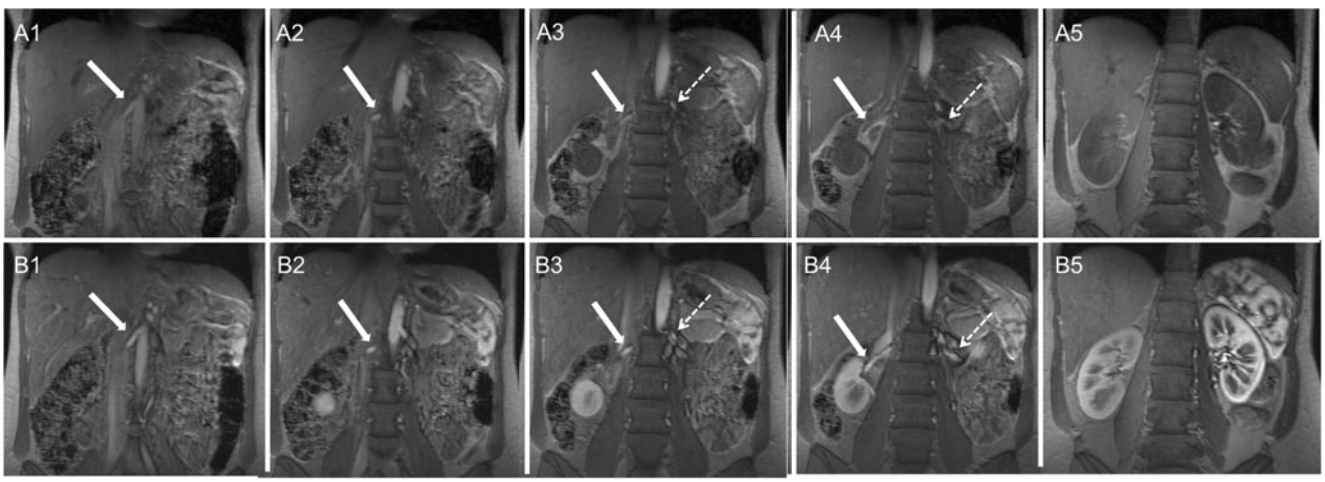

Fig. 3 Set of unenhanced (*A1–A5*) and contrast-enhanced (*B1–B5*) 3D FLASH MRAs in the same subject. The *wide arrows* point at the right renal artery, demonstrating strong improvement after the application of contrast agent in the depiction of peripheral vessel segments (*B4*). *Dashed arrows* point at the left renal artery (*A3–A4* and *B3–B4*)

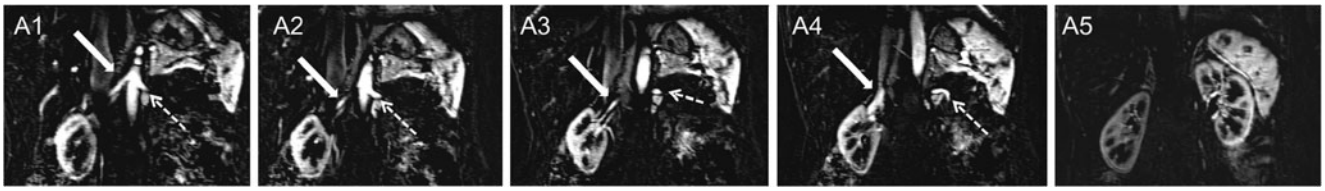

Fig. 4 Set of subtraction images with the *wide arrow* pointing to the right and the *dashed arrow* pointing to the left renal artery

33.8) and the distal segments of the right renal artery (mean increase 33.8). SNR measurements showed the smallest increase in the abdominal aorta ($mean_{unenhanced}$ 66.6 to $mean_{contrast\text{-}enhanced}$ 93.3).

As indicated by the SNR measurements, CNR measurements accordingly yielded a strong increase after the application of contrast agent with an average increase of 58.1 %, yet also showing statistical significance in all vessel segments. Corresponding to the increase in SNR, the strongest increase in CNR (p=0.041) was detected for the distal segment of the left renal artery, which had the smallest unenhanced CNR value of all vessel segments of 17.8 ($mean_{contrast\text{-}enhanced}$ 59.7). Similar increases were achieved for the proximal segment of the left renal artery ($mean_{unenhanced}$ 20.5 to $mean_{contrast\text{-}enhanced}$ 50.8; p=0.043) and the distal segments of the right renal artery ($mean_{unenhanced}$ 27.7 to $mean_{contrast\text{-}enhanced}$ 56.9; p=0.045) (Fig. 7). The application of contrast agent yielded the mildest CNR increase for the abdominal aorta with an average value of 21.9.

Discussion

This pilot study of first-pass contrast-enhanced 7-T MRA of the renal arteries demonstrates the feasibility of this imaging technique as well as the limitations and challenges associated with the physical changes at ultra-high magnetic field strength.

While DSA remains the gold standard for the assessment of renal artery lesions, contrast-enhanced MR angiography has established itself as an excellent, non-invasive diagnostic alternative for vessel imaging, demonstrating its diagnostic superiority and/or equivalence to other imaging techniques such as ultrasound or CT [1, 2]. An increase in the magnetic field strength to 3 T has been demonstrated to be beneficial for MR angiographic applications owing to various physical effects [15]. First, the affiliated increase in SNR can be traded off in variations of spatiotemporal resolution: the spatial resolution can be improved at a given acquisition time, the acquisition time can be shortened at a given spatial resolution, or both parameters can be adjusted [6, 16]. Additionally, T1 times of surrounding tissue are prolonged by 10 % to 20 % compared with blood [16]. Thus, based on the decreased relaxation rate, fast repetitious RF excitations result in improved vessel-to-background contrast [15]. Although these characteristics have been shown to be technically beneficial for 3-T MRA, a clear diagnostic advantage has not yet been shown [17].

However, a further increase in the magnetic field strength beyond 3 T bears the potential for an exacerbation of artefacts and impairing changes due to physical effects. Previous studies of ultra-high-field abdominal MRI have shown

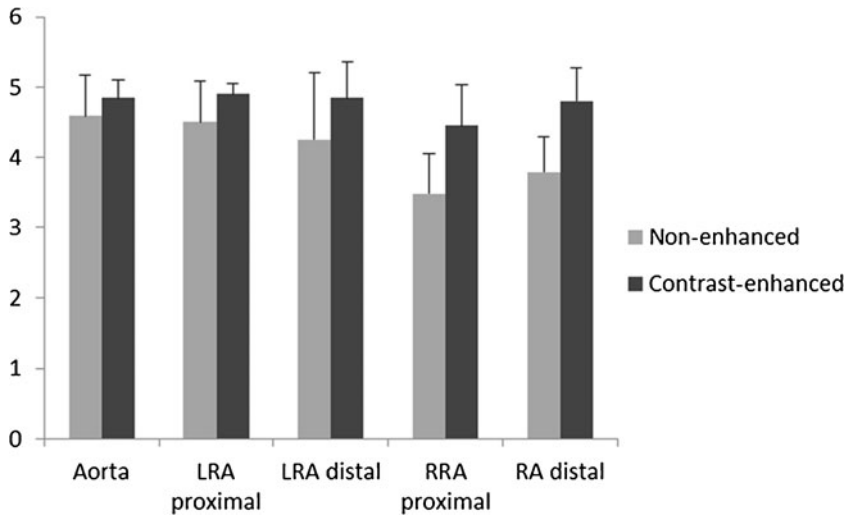

Fig. 5 Mean values and standard deviation of qualitative image analysis of the delineation of the abdominal aorta and renal arteries. Scoring results demonstrate the improved delineation of all the vessel segments assessed after the application of contrast agent. LRA = left renal artery; RRA = right renal artery

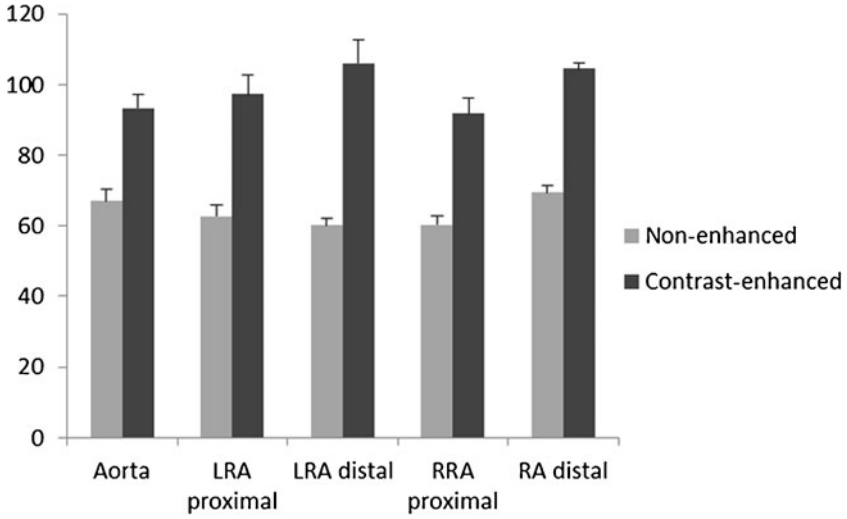

Fig. 6 Mean values and standard deviation of quantitative image analysis of SNR of the abdominal aorta and renal arteries. The results show the strongest improvement after the application of contrast agent for the left distal renal artery and equally strong improvement in SNR for the left proximal and right distal renal artery segments. LRA = left renal artery; RRA = right renal artery

impairments due to signal intensity variations across the image based on the shortening of the RF wavelength and concomitant RF heterogeneities [6–8]. Despite the application of B_1 shimming with a custom eight-channel B_1 shimming set up, minor shortcomings due to B_1 artefacts persisted [6–8]. In our study set up we applied a phase increment of 45° and equal amplitudes (conventional CP^+ mode) between neighbouring elements to successfully transition residual B_1 signal voids out of the region of interest and into the right upper quadrant of the abdomen. This strategy worked because we were only interested in a limited region of interest near the centre of the field of view, which included the renal arteries and perirenal aorta.

Furthermore, MRA sequences at high field strengths are known to be restricted by specific absorption rate limitations because of the short repetition times, fairly high flip angles, and the increase in the energy deposition in tissue with the square of the field strength. To compensate for the energy deposition, parallel imaging can be applied to limit the requisite number of k-space lines. The utilisation of parallel imaging can also improve the spatiotemporal resolution while maintaining anatomical coverage, which is a challenging issue in breath-hold bolus imaging techniques. The loss in SNR due to parallel imaging may be counterbalanced by the inherent gain in SNR at higher magnetic field strengths [16]. Nevertheless, because of SAR limitations and the temporal constraint of 20 s maximum for breath-hold imaging, the spatial resolution in our trial remained restricted to a voxel size of $1.0 \times 1.5 \times 1.0$ mm^3.

First studies on 7-T unenhanced brain imaging revealed an incidental finding that enhances the potential for unenhanced MRA, yet may also impede the acquisition of high-quality contrast-enhanced MRA. These initial studies demonstrated an inherently hyperintense signal of the arterial vasculature in T1-weighted unenhanced imaging [6, 9]. First study results have demonstrated the potential for 7-T unenhanced MR angiographic applications, applying MPRAGE or 3D VIBE imaging [9, 18]. The inherently positive vessel-

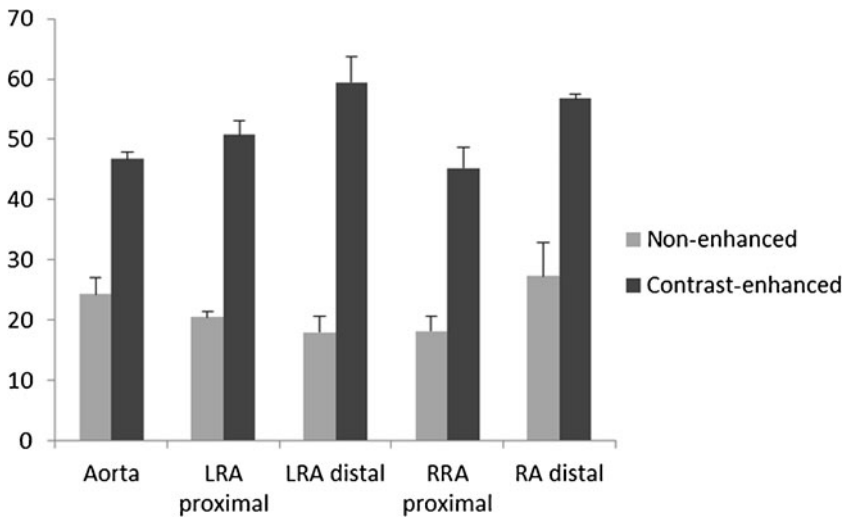

Fig. 7 Mean values and standard deviation of quantitative image analysis of CNR of the abdominal aorta and renal arteries in correlation with the adjacent major psoas muscle. While the strongest improvement in CNR is revealed on contrast-enhanced images for the distal segments of the left renal artery, the smallest improvement was detected for assessment of the abdominal aorta. LRA = left renal artery; RRA = right renal artery

to-background contrast at 7 T has also been observed in initial approaches to unenhanced 7-T abdominal MRI [6]. The aetiology of the inherently high vascular T1 signal is incompletely understood so far. However, a combination of steady-state and inflow effects seems to be responsible, as flowing spins are not pre-saturated by RF pulses when entering the imaging region because of the utilisation of local transmit RF coils at ultra-high-field abdominal MRI [18]. Furthermore, the utilisation of local transmit coils at 7 T also seems to be accountable for the high signal intensity in MPRAGE, as this means that a non-selective inversion recovery pulse is effectively slab-selective [18]. The imaging results in our trial confirm the excellent delineation of unenhanced arterial vasculature due to the homogeneous hyperintense vessel signal, enabling high-quality unenhanced angiographic imaging of the renal arteries. Metzger et al. presented initial study results demonstrating the feasibility of unenhanced 7-T renal MRA [10, 19]. Via utilisation of targeted B1 shimming based on small flip calibration images, the good-qualtiy visualisation of both renal arterial branches was possible.

Nevertheless, the application of contrast agent is a prerequisite for the acquisition of fast contrast-enhanced MR angiography sequences. Hence, this feasibility trial is of particular interest as the application of gadolinium-based contrast agent has been introduced in only a very limited number of ultra-high-field extracranial studies [6, 8]. Despite the inherently hyperintense vessel signal, our results showed an improvement in vessel delineation after the application of contrast agent, reflected in both qualitative and quantitative image analysis. To further optimise subtraction imaging, in which the unenhanced data are subtracted from the contrast-enhanced data to increase the benefit of contrast enhancement, complete suppression of the unenhanced vessel signal would have been desirable. However, the approaches using two sinc-shaped 90° RF pulses employing the VERSE algorithm to saturate the inherently high vessel signal remained unsatisfying, as only the signal of the upper and lower portions of the abdomen could be partially saturated, leaving the renal arterial vessel signal hyperintense.

As demonstrated in prior trials, an increase of the magnetic field strength is associated with a decrease in relaxivity [20, 21]. Rohrer et al. and Noebauer-Huhmann et al. investigated changing magnetic properties of MRI contrast agents with increasing field strength from 1.5 T to 4.7 T and 3 T to 7 T, respectively. Yet, currently, there are no published data on human in vivo r1 relaxivity changes in gadolinium-based contrast agents at higher magnetic field strengths and only very limited data on in vitro changes [20]. Hence, we decided to administer the standard dosage for gadobutrol of 0.1 mmol/kg bodyweight in this initial feasibility trial. In accordance with the potential reduction of contrast agent dosage for 3-T vessel imaging [15], a further decrease in the gadolinium dosage needed at 7 T should be investigated in future clinical studies.

In conclusion, to our knowledge, this is the first study demonstrating the feasibility of contrast-enhanced renal MRA at ultra-high magnetic field strength, including a comparison with unenhanced MRA. Despite the high quality of unenhanced renal MRA, qualitative and quantitative results demonstrated a further improvement in vessel assessment after the application of contrast agent. Known impairments due to B_1 field heterogeneities could be reduced, transitioned out of the defined region of interest. Further improvements in RF excitation techniques as well as patient studies with renal arterial abnormalities should be the focus of future studies to investigate additional diagnostic benefits associated with ultra-high magnetic field strength.

References

1. Soulez G, Pasowicz M, Benea G et al (2008) Renal artery stenosis evaluation: diagnostic performance of gadobenate dimeglumine-enhanced MR angiography comparison with DSA. Radiology 247:273–285
2. De Cobelli F, Venturini M, Vanzulli A et al (2002) Renal arterial stenosis: prospective comparison of color Doppler US and Breath-hold, three-dimensional, dynamic, gadolinium-enhanced MR angiography. Radiology 214:373–380
3. De Cobelli F, Vanzulli A, Sironi S et al (1997) Renal artery stenosis: evaluation with breath-hold, three-dimensional, dynamic, gadolinium-enhanced versus three-dimensional, phase-contrast MR angiography. Radiology 205:689–695
4. Willmann JK, Wildermuth S, Pfammatter T et al (2003) Aortoiliac and renal arteries: prospective intraindividual comparison of contrast-enhanced three-dimensional MR angiography and multi–detector row CT Angiography. Radiology 226:798–811
5. Michaely HJ, Kramer H, Dietrich O et al (2007) Intraindividual comparison of high-spatial-resolution abdominal MR angiography at 1.5 T and 3.0 T: initial experience1. Radiology 244:907–913
6. Umutlu L, Orzada S, Kinner S et al (2010) Renal imaging at 7 Tesla: preliminary results. Eur Radiol 21:841–849
7. Umutlu L, Kraff O, Orzada S et al (2011) Dynamic contrast-enhanced renal MRI at 7 Tesla: preliminary results. Invest Radiol 46:425–433
8. Umutlu L, Bitz AK, Maderwald S et al (2012) Contrast-enhanced ultra-high field liver MRI: a feasibility trial. Eur J Radiol. doi:10.1016/j.ejrad.2011.07.0049
9. Maderwald S, Ladd S, Gizewski E et al (2008) To TOF or not to TOF: strategies for non-contrast-enhanced intracranial MRA at 7 T. Magnet Reson Mater Phys, Biol Med 21:159–167
10. Metzger GJ, Simonson J, Bi X (2010) Initial experience with non-contrast enhanced renal angiography at 7.0 Tesla. Proceedings of the 18th Annual Meeting of ISMRM, Sweden (Abstract 403)
11. Orzada S, Quick HH, Ladd ME, et al (2009) A flexible 8-channel transmit/receive body coil for 7 T human imaging. Proceedings of the 17th Annual Meeting of ISMRM, Honolulu, HI, USA (Abstract 2999)
12. Bitz A, Brote I, Orzada S, et al (2009) Am 8-channel add-on RF shimming system for whole-body 7 Tesla MRI including real-time SAR monitoring. Proceedings of the 17th Annual Meeting of ISMRM, HI, USA (Abstract 4767)

13. Christ A, Kainz W, Hahn EG et al (2010) The Virtual Family —development of anatomical CAD models of two adults and two children for dosimetric simulations. Phys Med Biol 55: N2–N38
14. Conolly S, Nishimura D, Macovski A (1988) Variable-rate selective excitation. J Magn Reson 78:440–458
15. Michaely HJ, Kramer H, Attenberger U et al (2007) Renal magnetic resonance angiography at 3.0 T: technical feasibility and clinical perspectives. Top Magn Reson Imag 18:117–125
16. Fenchel M, Nael K, Deshpande VS et al (2006) Renal magnetic resonance angiography at 3.0 Tesla using a 32-element phased-array coil system and parallel imaging in 2 directions. Investig Radiol 41:697–703
17. Willinek WA, Born M, Simon B et al (2003) Time-of-flight MR angiography: comparison of 3.0-T imaging and 1.5-T imaging—Initial experience. Radiology 229:913–920
18. Grinstead JW, Rooney W, Laub G (2010) The origins of bright blood MPRAGE at 7 Tesla and a simultaneous method for T1 imaging and non-contrast MRA. Proc Intl Soc Mag Reson Med 18:(Abstract 1429)
19. Metzger GJ, van de Morteele PF (2011) Non-contrast enhanced renal MRA at 7 T. Proc Intl Soc Mag Reson Med 19. (Abstract)
20. Noebauer-Huhmann IM, Szomolanyi P, Juras V et al (2010) Gadolinium-based magnetic resonance contrast agents at 7 Tesla: in vitro T1 relaxivities in human blood plasma. Invest Radiol 45:554–558
21. Rohrer M, Bauer H, Mintorovitch J et al (2005) Comparison of magnetic properties of MRI contrast media solutions at different magnetic field strengths. Invest Radiol 40:715–724